Indian Journal of Pure & Applied Physics
Vol. 61, October 2023, pp. 823-829
DOI: 10.56042/ijpap.v61i10.319

Annealing-assisted SnO_2 Thin Film for Selective Hydrogen Gas Sensor

Vipin Kumar[a], Yogendra K Gautam[a]*, Ravikant Adalati[b], Ashwani Kumar[b,c]*, Beer Pal Singh[a], Satyendra Kumar Mourya[d], Harish Verma[e] & Mukesh Jangir[f]

[a]Smart Materials and Sensor Laboratory, Department of Physics, Chaudhary Charan Singh University Campus Meerut, Uttar Pradesh 250 004, India

[b]Institute Instrumentation Centre, Indian Institute of Technology Roorkee, Uttrakhand 247 667, India

[c]Department of Physics, Graphic Era (Deemed to be University), Dehradun, Uttarakhand 248 002, India

[d]Department of Electrical and Electronics Engineering, Birla Institute of Technology and Science Pilani, Pilani 333 031, Rajasthan, India

[e]Department of Physics, Indian Institute of Technology (B.H.U), Varanasi, Uttar Pradesh 221 005, India

[f]School of Applied Sciences and technology, Chemistry Department, NIMS University, Jaipur, Rajasthan 303 121, India

Received 18 April 2023; accepted 16 August 2023

Today, monitoring and classification of hydrogen gas by metal oxide-based sensors are widely studying to improve their selectivity and stability. In present work, hydrogen sensing properties of magnetron sputtered deposited pure SnO_2 thin films have been studied. The pure SnO_2 thin film was deposited on glass substrate and as-deposited film was annealed at 450 °C for 6 hrs. The annealed SnO_2 thin film has crystalline tetragonal structure, granular surface morphology and non-stoichiometry elemental composition of tin and oxygen vacancies. A higher gas sensing response is obtained for annealed SnO_2 thin film as compare to as-deposited SnO_2 thin film.A limit of detection (LOD) ~175 ppb is estimated for annealed SnO_2 thin film-based sensor. This sensor exhibits fast response and recovery time of 42 s/52 s for 50 and 500 ppm hydrogen gas, respectively. The sensor is found highly selective towards H_2 gas in compare to different gases such as methane, carbon monoxide and nitrogen dioxide.

Keyword: Hydrogen; Gas sensors; SnO_2 thin films; Sputtering; FE-SEM; Selectivity

1 Introduction

Now adays, there is wide attention in evolving consistent hydrogen (H_2) gas sensors for noticing ppm level volume with a great response and a fast working time. Semiconductor oxide nanostructures like as SnO_2 and ZnO are the most frequently used because of their non-stoichiometry properties, which perform the adsorption of air oxygen onto their structure, which are suitable for searching to different combustible and poison gases[1]. Thin film morphology dependent gas sensors, such as nanorod, nanowires and nanotubes have broadly great sensitivity response, but currently their manufacturing rate in laboratories or industry for commercialization very expensive and large time consume because manufacturing technique limited and expensive[2]. The most studied hydrogen gas sensors are based on 2D-thin film because of their simple structure, conformation and accessible manufacturing for commercialization and low fabrication cost and time. These type of gas sensors are generally manufactured by different techniques, for examples, atomic layer deposition[3], e-beam evaporation[4] and sputtering[5-7]. The sputtering route has some advantages such as uniformity, adhesive and purity, *etc*[8]. The SnO_2 based nanostructured perform low sensitivity at low temperatures[9–13]. Mostly, these types of sensors work in the operating temperature range of 200–250 °C[9,11,14]. The higher response was achieved at even or beyond 300 °C[15–18]. There are several reports available in literature on the SnO_2 based nanomaterial with good sensing response towards various gases and organic vapors. Yamazoe & Shimanoe have reported structural quality of the nanomaterial such as grain size, sensing layer thickness, porosity and morphology *etc*. for optimization MOS nanostructures to increase sensitivity and selectivity[19]. Masuda reported that the SnO_2 film thickness is a important factor to detect low-ppm amount of gas, small thickness (few nm) of sensing layers detect low ppm of gas easily. Therefore, the development of SnO_2 sensors has been interesting devotion since last few years with enhanced gas sensing performance[20]. Yang *et al*., and

*Corresponding authors:
(E-mail: ykg.iitr@gmail.com; akumar1@ic.iitr.ac.in)

others achieved higher hydrogen gas sensing response for annealed MOS-based sensors[21-28].

In this present work, the effect of annealing temperature on structural, morphological and gas sensing properties of SnO_2 thin film is investigated.

The annealed SnO_2 thin film shows high selectivity and stability towards low concentration of H_2 gas. The H_2 gas sensing mechanism of SnO_2 thin film sensor is also explained.

2 Experimental Section

2.1 Materials

The SnO_2 thin film was deposited on a cleaned glass (soda lime) substrate using RF- reactive sputtering with Tin (2 inch diameter, 4 mm thickness) sputtering targets with 99.99% purity. All the materials were procured from Soleras Advanced Coatings, Shanghai, China. Argon (Ar), oxygen (O_2), synthetic air, Hydrogen (H_2), Nitric oxide (NO_2), Ammonia (NH_3) and Carbon mono oxide (CO), all 99.99% pure gases were purchased from Sigma Gases, India.

2.2 Sensor Fabrication Process

The as-deposited SnO_2 thin film was prepared on glass substrates. The substrate was cleaned with laboratory reagents and ultrasonically cleaned for 30 minutes at room temperature and dried at 100 °C for 20 minutes. The glass substrate was placed in the sputtering chamber at a distance of 8cm from the Tin (Sn) target. The sputtering chamber was evacuated to a pressure of 6.6×10^{-6} mbar by a turbo molecular pump backed by a rotary pump. The constant flow of Ar and O_2 gases was introduced into the chamber in the required manner. During the sputtering deposition process, working pressure was kept fixed at 4.1×10^{-2} (mbar). The SnO_2 thin film was deposited on glass substrate ($1\times 1\ mm^2$size) at room temperature, the as-deposited film was annealed at 450 °C for 6 hours in a tubular furnace to achieve crystalline film structure. The as-deposited SnO_2 and annealed SnO_2 thin film samples are named as T1 and T2 sensor, respectively. The detailed deposition parameters are given in Table-1.

2.3 Characterization

The structure of as-deposited and annealed SnO_2 thin film was analyzed using an X-ray diffractometer (Bruker AXS, D8 Advance) with (2θ) geometry. The morphology was analyzed by field emission scanning electron microscope (FE-SEM) (Carl Zeiss). The elements in percentage (%) was analyzed by energy dispersive X-ray analysis (EDAX).

2.4 Sensor Gas Testing

Hydrogen gas sensing tests were carried out in a stainless-steel, custom made (Excel Instruments Mumbai, India) chamber, equipped with a PID controlled electric heater, allowing measurements in controlled atmosphere. Before the sensing measurements, the chamber of sensing setup was evacuated to 7 mbar with a rotary pump. The desired concentration of H_2 gas and other gases were introduced for the sensing measurement. The response of sensors were measured using source-current-meter and voltmeter (Keithley 2450) with two probes as shown in Fig. 1. The sensor response was calculated by following Eq. 1:

$$R = \frac{R_a}{R_g} \quad ...\ (1)$$

Here,R_a and R_g are the measured resistances of the sensors in air and target gas, respectively.

3 Results and Discussion

3.1 Structures Analysis

The XRD patterns as-deposited and annealed SnO_2 thin films are shown in Fig. 2. It is found there is structural transition from an amorphous structure phase to a tetragonal crystal structure phase upon annealing of as-deposited SnO_2 thin film. For the annealed SnO_2 thin film, diffraction peaks are observed corresponding to (110), (111), and (211) planes at angles of 27.36°, 38.8°, and 52.46°, respectively, as per JCPDS ICDD no. 41-1445[29]. Remarkably, the average crystallite size of the annealed SnO_2 thin film was calculated using the Scherrer formula Eq. 2[30].

$$(D)= \frac{0.94\times\lambda}{\beta\times cos\theta} \quad ...\ (2)$$

Table 1 — Deposition and annealing parameters.

1.	Target	Sn
2.	Substrate	Glass
3.	Base Pressure (mbar)	6.6×10^{-6}
4.	Working Pressure (mbar)	4.1×10^{-2}
5.	Power (RF)	100W
6.	Ar +O_2 flow (sccm)	30:5
7.	Target to Substrate Distance	8 cm
8.	Time of Deposition	30 minute
9.	Post thermal annealing	450°C for 6 hour

Table 2 — Grain size, lattice strain, dislocation density, inter-planar distance, lattice constant of T2 sensor.

Sensor	Crystallites size (nm)	Lattice strain (ε)	Dislocation density (δ) Line/m^2	Interplanar distance d (Å)	Lattice constant (a=b)	Lattice constant (c)	Lattice deformation a/c
T2	10	1.27	0.019	3.03	4.792	3.479	1.377

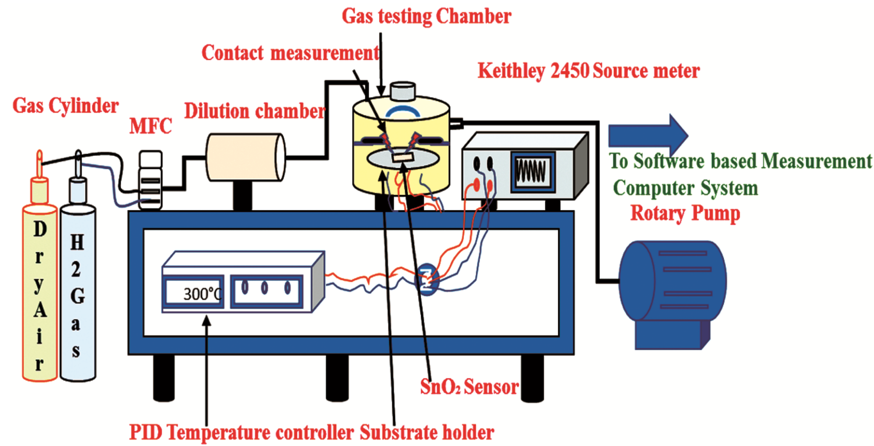

Fig. 1 — The gas sensing system.

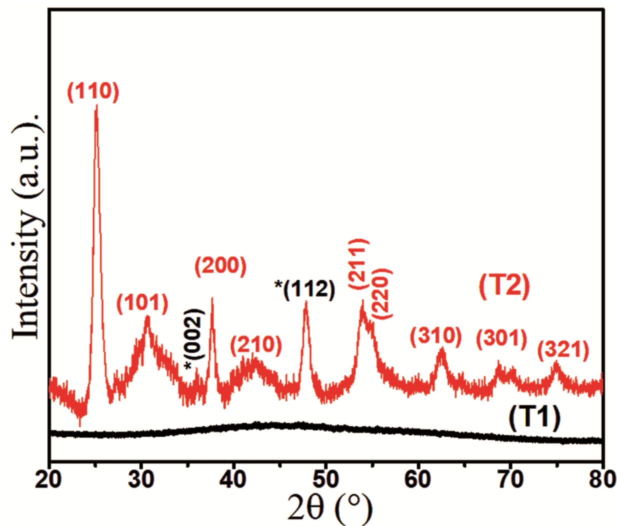

Fig. 2 — XRD patterns of SnO_2thin films-based sensors: (T1) as-deposited and (T2) annealed.

and it was found to be ~10 nm. The strain of thin film was calculated by Eq. 3[31].

$$(\varepsilon) = \frac{\beta}{4tan\theta} \quad ... (3)$$

This strain arises due to structural transformations that can introduce defects such as dislocations and grain boundaries[32]. The dislocation densities $(\delta) = \frac{1}{D^2}$, significantly depend on the grain size and the presence of strains in the film which can have a detrimental effect on the sensing properties. A lower density of dislocations results less surface roughness, thereby providing more active sites for oxygen molecules to interact with target gas. The lattice constant of T2 sensor was found to near the standard value a = 4.76 Å, and c = 3.21Å and lattice deformation very less 1.37Å[32] Deepa *et al*., said that less lattice deformation sensor show higher response to a selective gas[32]. The crystallite size, strain, and dislocation densities of T2 thin film sensor are tabulated in Table 2.

3.2 Surface morphology and EDAX analysis

The high-magnification FE-SEM images of the as-deposited and annealed SnO_2 thin film, are shown in Fig. 3(a,c), respectively. A cross-sectional view is shown in Fig. 3(b) and thickness of T2 thin film sensor was found to be~334 nm. These SnO_2 thin films exhibit a uniform, dense and nano-granular morphology[30]. The Fig. 3(d,e), show element distribution of Sn and O in SnO_2 thin films. The presence of Sn and O elements in SnO_2 thin films are also confirmed by EDAX spectra as shown in Fig. 4(a,b). It is noteworthy that both thin films exhibit a non-stoichiometric composition of Tin and Oxide[1], as the atomic percentage ratio of [O]/[Sn] = 5.74 were observed[1].

3.3 Sensor Characteristics

The operating temperature of n-type semiconductor gas sensors not only determines the species and existing forms of oxygen ions adsorbed on their surfaces, but it also has a direct impact on the reaction

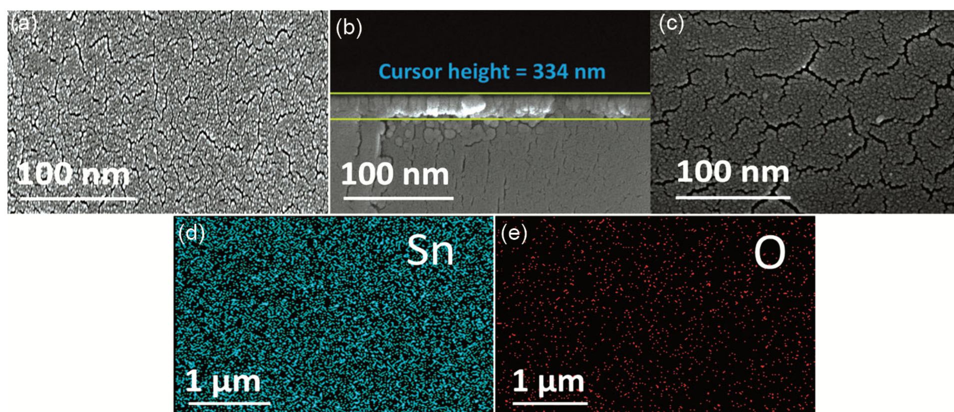

Fig. 3 — FESEMimages of: (a) As-deposited (T1) sensor, (b) cross-sectional view, (c) T2 sensor. EDS element distribution pattern of T2 sensor: (d)Sn element-dark blue and (e) oxide element-dark red .

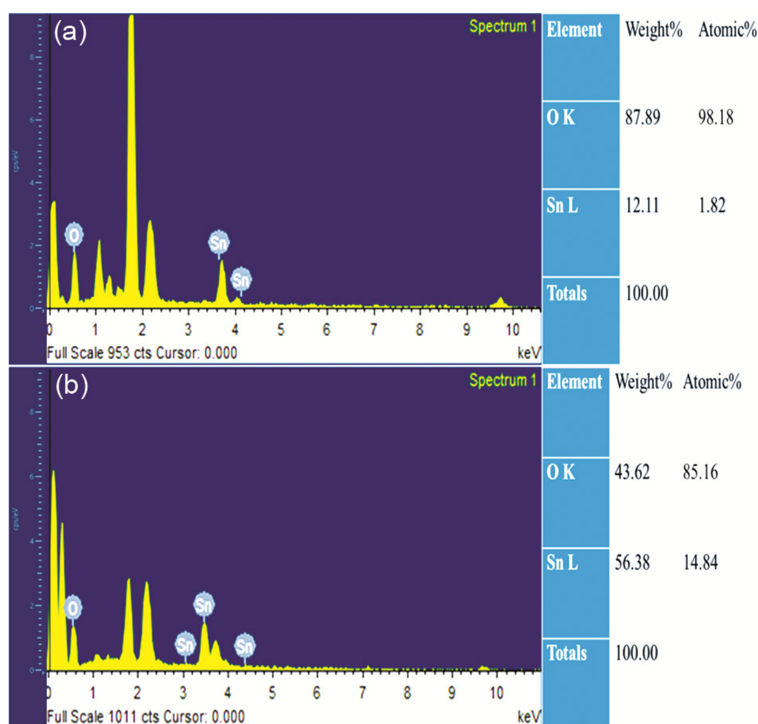

Fig. 4 — EDAX spectra: (a) T1 sensor and (b)T2 sensor.

and desorption process when the gas sensors come into contact with the target gas[29]. The power consumption, gas sensitivity and selectivity are strongly dependent on their working temperature. Fig. 5(a), depicts the sensor's response as a function of temperature. The H_2 gas sensor response was examined at operating temperature range 100 to 350 °C. The higher sensing response was noticed at 300 °C for both T1 and T2 sensors, which is defined as sensor working temperature. At lower temperature,the energy available at the surface is insufficient for the adsorption and dissociation of H_2 molecules. Also, the adsorption and conversion of atmospheric oxygen into (O^- orO_2^-) requires sufficient energy to occur[33]. At higher operating temperatures (>300 °C), the adsorbed gas has more energy to escape the surface before reacting with other adsorbed species to contribute to response.

Hence, the response decreases at much higher temperatures. T1 sensor has a very low response at all operating temperatures. The T2 sensor provides higher response. Many factors, including small grain, granular shape, and nonstoichiometric contribute to this sensing behavior[34,35]. The sensor T2 has a small grain size that results in higher initial resistance without exposure to H_2, which enhances the response

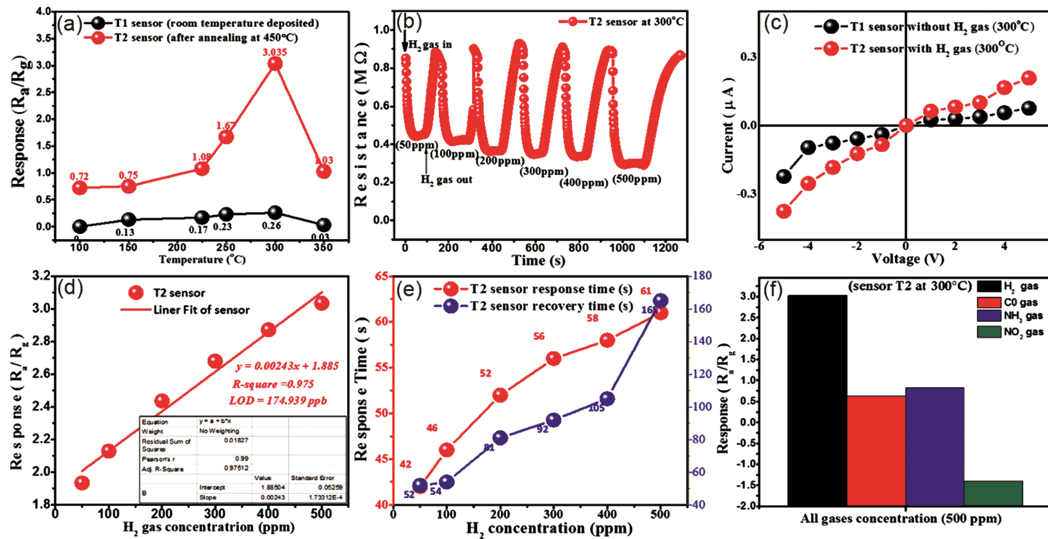

Fig. 5 — (a). Sensors response to H_2 gas 500 ppm concentration at variation of temperature (100-350 °C), (b). Transit response of sensor T2 at different ppm H_2 gas (temperature 300 °C), (c). Voltage-current (V-I) plot of T2 sensor at 300 °C in air and H_2 gas atmosphere, (d). Response Vs. H_2 gas concentration curve, (e). Transit response and recovery time plot of T2 sensor, (f). T2 sensor selective response in different gases.

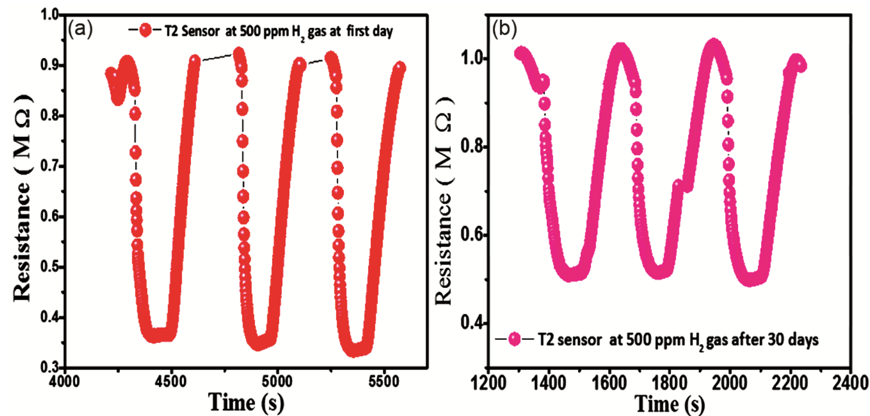

Fig. 6 — (a&b). Cyclic repeatability of T2 sensor at 500 ppm H_2 gas concentration for 30 days duration.

due to high active surface area. The T2 sensor's transit response to H_2 gas concentration curve for the gas concentration range of 50 to 500 ppm Vs. time (sec.) at 300 °C present 90% recovery as shown in Fig. 5(b). The sensor V-I curve shown linear behavior before and after H_2 gas, 500 ppm introduced (shows in Fig. 5(c)). The Fig. 5(d) shows relation between response and H_2 gas concentration (50 to 500 ppm). The Fig. 5(d), shows the linearity behavior (R^2 nearer to 1) and linear equation.The least detection limit (LOD) of T2 sensor is estimated ~175 ppb[36]. The Fig 5(e), shows the response/recovery time of the sensor T2, and it was found to be 42 s/52 s and 61 s/165 s at 50 and 500ppm H_2 gas, respectively. The sensor's response and recovery times, increase as H_2-gas concentration because conductance of the sensor increases as the number of free charge carriers grows[8]. Fig. 5(f) depicts the selectivity to hydrogen gas in the other gases atmosphere. The sensor response for gases, such as CO, NH_3, and NO_2, at 500 ppm concentration are found much lower than the response towards H_2 gas. The results analyzed and show that SnO_2 sensor exhibits a high response to hydrogen gas. This is because of lower instigation energy, size and weight of H_2 molecules. Thus H_2 gas is highly reactive to SnO_2 sensor and making it highly selectivity for hydrogen gas[36]. The result of repeatability test with three cycles at 500 ppm H_2 gas concentration, after 30 days duration is shown in Fig. 6. It is found that T2 sensor has strong stability with several cycles[37].

Table 3, presents a comparative analysis of several MOS-based hydrogen sensors[36-44].

Table 3 — Comparable study of different MOS-based hydrogen gas sensors.

	Sensors	Fabrication	Operating Temp. (°C)	Maximum response	Concentration (ppm)	Response and recovery time (sec.)	Ref.
1	Micro-sized Pd/SnO_2	sputtering	180	3	100	50/50 (50 ppm)	(38)
2	Au nanoparticles @ZnO	sputtering,Heat treatment	400	60*	600	252/639	(39)
3	Pt/TiO_2 thin film	flame-spray-made	300	470	10,000	8/~1000	(40)
4	Graphene-NiO thin films	modified hummers method	300	1.50	2000	57/28	(41)
5	NiO thin films	sputtering	175	1.68	3000	1000/1400	(42)
6	Pd/CuO thin film	sputtering	300	3.01	1000	10/50	(43)
7	Pd/SnO_2 nanoparticles	spin coating	RT.	1.2	1000	214/51.5	(44)
8	Pd/SnO_2 nanowires	thermal CVD/sputtering	150	4.5	100	>5/>6 min	(45)
9	WO_3 thin film	HFCVD	250	87*	100	3–4min/8–9 min	(46)
10	SnO_2 thin film	sputtering	300	3.04	50	42/52	This work

4 Sensing mechanism

Figure 7, explains the mechanism of n-type SnO_2 gas sensor to detect reducing gas environment, such as hydrogen gas. The change in the electrical resistance of as-deposited and annealed SnO_2 thin films with and without gas are examined[27]. The chemisorptions process of oxygen molecule types O_2^-, O^{2-} and $2O^-$ occurs by trapping electron on the SnO_2 surface (Fig. 7) at different temperature ranges, resulting in the creation of Schottky potential barrier height[27]. The chemisorptions process of oxygen molecule kinds of O_2^- and $2O^-$ takes place by capturing electron on the SnO_2 surface (Fig. 7) at different temperature ranges, which leads to Schottky potential barrier height formation. The reactions are represented by the following equations (eqns. 4-6)[45]:

$$O_{2(gas)} \rightarrow 2O_{(adsorbed)} \quad \ldots (4)$$

$$2O_{(adsorbed)} + e^- \rightarrow O^-_{2(adsorbed)} \text{ (T<100 °C)} \quad \ldots (5)$$

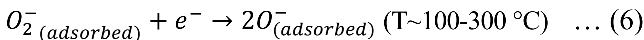

$$O^-_{2\,(adsorbed)} + e^- \rightarrow 2O^-_{(adsorbed)} \text{ (T~100-300 °C)} \quad \ldots (6)$$

When H_2 gas is introduced into the gas chamber, it reacts with surface adsorbed oxygen species (O^-), releasing an electron and the form a water molecule and barrier height down wards. This caused, as a result, the electrical resistance downward, which shows as a chemo-resistive response of sensor towards the gas. The reaction (7) take place as follows:

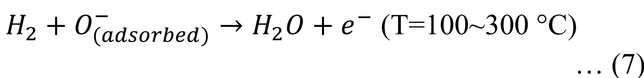

$$H_2 + O^-_{(adsorbed)} \rightarrow H_2O + e^- \text{ (T=100~300 °C)} \quad \ldots (7)$$

The small crystallite of SnO_2 thin film offers a higher surface area to perform effective reaction with the reducing gas. As a result, the interaction probability of gas molecules with active surface sites increases and provides a higher response.

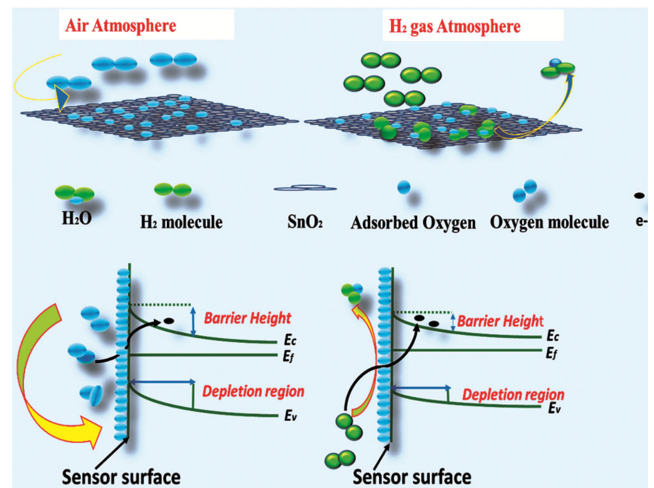

Fig. 7 — Schematic representation of T2 sensor in air and H_2 gas atmosphere.

In the air environment, oxygen atoms are adsorbed on the surface of the SnO_2 thin film, establishing an electron depletion region. Under exposure to H_2 gas, the electrons transferred from the oxygen adsorbed on the SnO_2 surface to the H_2 molecules, decreases the electron depletion width[29]. Several reports recommend that the electron depletion length should be around 3 to 3.25 nm for SnO_2 to initiate chemisorption. In this study, the sensor shows higher response due to the lower average crystallite of 10 nm[27,45-49]. Another important factor for improvement in the H_2 gas sensing properties is related with improvement in the non-stoichiometry ratio of the sensing materials after annealing[50].

5 Conclusion

The magnetron sputtered pure SnO_2 thin film was annealed to obtain its crystalline structure with granular morphology. The annealed SnO_2 thin film sensor presents excellent hydrogen gas sensing response. The sensor shows fast response/recovery time of 42/52 and

61/165, respectively for 50 and 500 ppm concentration of hydrogen gas. The sensor was found selective towards hydrogen gas and stable for longer duration of one month. The studied pure SnO_2 thin film can be utilized to design H_2 gas sensor even without using any expensive catalytic layer (Pd, Pt, Au).

Acknowledgment

The authors would like to thank Prof. Ramesh Chandra, IIC, IIT Roorkee, India, for providing, XRD and FE-SEM facilities to carry out this research work. The authors also thank DST, Govt. of India, for providing a FIST grant for sputtering. This work was supported by the UGC, Govt. of India [No.F.30-303/2016 (BSR) and F.D.Dy. No. 11299], and CCS University, Meerut [DEV/URGS/2022-23/39]

References

1 Chu J, Peng X, Wang Z & Feng P, *J Mater Res Bull*, 47 (2012) 4420.
2 Duy N Van, Hoa N D & Hieu N Van, *J Sens Actuators B: Chem*, 173 (2012) 211.
3 Boyadjiev S I, Georgieva V, Yordanov R, Raicheva Z & Szil Agyi I M, *Appl Surf Sci*, 387 (2016) 1230.
4 Wisitsoraat A, Tuantranont A, Patthanasettakul V, Lomas T & Chindaudom P, *J Sci Technol Adv Mater*, 6 (2005) 261.
5 Goudarzi S & Khojier K, *AIP Conf Proc*, 1920 (2018) 20049.
6 Sberveglieri G, *J Sens Actuators B: Chem*, 23 (1995) 103.
7 Yang W, Gan L, Li H & Zhai T, *Inorg Chem Front*, 3 (2016) 433.
8 Sanger A, Kumar A, Kumar A & Chandra R, *Sens Actuators B: Chem*, 234 (2016) 8.
9 Zhang B W, Fu W Y, Li H Y, Fu X L, Wang Y, Bala H, Wang X D, Sun G, Cao J L & Zhang Z Y, *J Appl Surf Sci*, 363 (2016) 560.
10 Wang Y L, Liu C, Wang L, Liu J, Zhang B, Gao Y, Sun P, Sun Y F, Zhang T & Lu G Y, *J Sens Actuators B: Chem*, 240 (2017) 1321.
11 Zhao Y P, Liu Y X, Ma Y X, Li Y H, Zhang J H, Ren X P, Li C, Zhao J C, Zhu J & H Y Zhao, *J ACS Appl Nano Mater*, 3 (2020) 7720.
12 Cheng L, Ma S Y, Wang T T, Li X B, Luo J, Li W Q, Mao Y Z & Gz D J, *J Mater Lett*, 131 (2014) 23.
13 Wang B, Sun L & Wang Y D, *J Mater Lett*, 218 (2018) 290.
14 Wang S J, Yu W W, Cheng C W, Zhang T N, Ge M Y, Sun Y & Dai N, *J Mater Res Bull*, 89 (2017) 267.
15 Umar A, Ammar H Y, Kumar R, Ibrahim A A & Al-Assiri M S, *J Sens Actuators B: Chem*, 304 (2020) 11.
16 Jiang X H, Ma S Y, Sun A M, Zhang Z M, Jin W X, Wang T T, Li W Q, Xu X L, Luo J, Cheng L, Mao Y Z & Zhang M, *J Appl Surf Sci*, 355 (2015) 1192.
17 Tan W H, Yu Q X, Ruan X F & Huang X T, *J Sens. Actuators B: Chem*, 212 (2015) 47.
18 Xu M H, Cai F S, Yin J, Yuan Z H & Bie L J, *J Sens Actuators B: Chem*, 145 (2010) 875.
19 Yamazoe N & Shimanoe K, 1 - Fundamentals of semiconductor gas sensors, in: Jaaniso R & Tan O K (Eds), Semiconductor Gas Sensors, Woodhead Publishing, (2013) 34.
20 Masuda Y, *Sens Actuators B: Chem*, 364 (2022) 131876.
21 Yang Y, Maeng B, Jung D G, Lee J, Kim Y, Beom J, Kwon H, Kyung A & Daewoong J, *J Nanomater*, 12 (2022) 3227.
22 Aragón F F H, Aquino J C R, Ardisson J D & Coaquira J A H, *J Mater Sci Semicond Process*, 93 (2019) 182.
23 Pakiyaraj K & Kirthika V, *J Nano Sci Technol*, 7 (2021) 949.
24 Cynthia S R, Sivakumar R, Sanjeeviraja C, Gopalakrishnan C & Jeyadheepan K, *J Appl Mater Sci*, 217 (2020) 2000512.
25 Yuan W, Liu X, Fang Z, Ning H, Zhang X, Deng Y, Deng P, Liang Z, Yao R & J Peng, *J Mol Cryst Liq Cryst*, 676 (2018) 44.
26 Zhu S, Tian Q, Wu G, Bian W, Sun N, Wang X, Li C, Zhang Y, Dou H, Gong C, Dong X, Sun J, An Y, Jing Q & Liu B, *Int J Hydrogen Energy*, 47 (2022) 17821.
27 Drmosh Q A, Yamani Z H, Mohamedkhair A K, Hendi A H Y & Ibrahim A, *J Vacuum*, 156 (2018) 68.
28 Toan N V, Hung C M, Hoa N D, Duy N Van, Le D T T, Hoa N T T, Viet N N, Phuoc P H, Hieu N V, *J Hazard Mater*, 3894 (2021) 00144.
29 Li A, Zhao S, Bai J, Gao S, Wei D, Shen Y, Yuan Z & Meng F; *J Sens Actuators: B. Chem*, 355 (2022) 131261.
30 Abinaya M, Pal R & Sridharan M, *J Solid State Sci*, 95 (2019) 105928.
31 Musa A M M, Farhad S F U, Gafur M A & Jamil A T M K, *J AIP Adv*, 11 (2021) 115004.
32 Deepa S, Kumari K P & Thomas B, *Ceram Int*, 8842 (2017) 32063.
33 Sanger A, Kumar A, Kumar A, Jaiswal J, Chandra R, *J Sens Actuators B: Chem*, 236 (2016) 16.
34 Hu D, Han B, Han R, Deng S, Wang Y, Li Q, et al, *J Chem*, 38 (2014) 2443.
35 Kumar M, Mehta B R, Singh V N, Chatterjee R, Milikisiyants S, Lakshmi K V, et al., *J Appl Phys Lett*, 96 (2010) 123114.
36 Kumar V, Gautam Y K, Gautam D, Kumar A, Adalati R & Singh B P, *J Fuels*, 4 (2023) 279.
37 Paul R, Das B & Ghosh R, *J Alloys Compd*, 941 (2023) 168943.
38 Duy N V, Toanb T H, Hoa N D & Hieu N V, *Int J Hydrogen Energy*, 40 (2015) 12572.
39 Drmosh Q A & Yamani Z H, *Appl Surf Sci*, 375 (2016) 57.
40 Chomkitichai W, Ninsonthi H, Liewhiran C, Wisitsoraat A, Sriwichai S & Phanichphant S, *J Nanomater*, (2013).
41 Kamal T, *J Alloy Comp*, 729 (2017) 1058.
42 Chou P C, Chen H I, Liu I P, Chen C C, Liou J K, Hsu K S & Liu W C, *Int J Hydrog Energy*, 40 (2015) 729.
43 Yadav P, Kumar A, Sanger A, Gautam Y K & Singh B P, *J Electron Mater*, 50 (2021) 192.
44 Kadhim I H, Hassan H H & Abdullah Q N, *J Nano-Micro Lett*, 8 (2016) 20.
45 Kien N, Hung C M, Ngoc T M, Le D T T, Hoa N D, Duy N V & Hieu N, *J Sens Actuators B Chem*, 253 (2017) 156.
46 Godbole R, Ameen S, Nakate U T, Akhtar M S & Shin H S, *J Mater Lett*, 254 (2019) 398.
47 Duy N V, Thai N X, Ngoc T M, Le D T T, Hung C M, Nguyen H, Tonezzer M, Hieu N V & Hoa N D, *J Sens Actuators: B Chem*, 351 (2022) 130979.
48 Wang R H, Wen W, Zheng S, Ye Z & Wu J-M, *Sens Actuators B: Chem*, 362 (2022) 131805.
49 Alenezi M R, Alzanki T H, Almeshal A M, Alshammari A S, Beliatis M J, Henley S J, et al., *RSC Adv*, 5 (2015) 103195.
50 Zhang T, Liu L, Qi Q, Li S & Lu G, *Sens Actuators B: Chem*, 139 (2009) 287.